

## Broadband all-optical ultrasound transducers

Yang Hou<sup>a)</sup> and Jin-Sung Kim

*Department of Electrical Engineering and Computer Science, University of Michigan, Ann Arbor, Michigan 48109*

Shai Ashkenazi and Sheng-Wen Huang

*Department of Biomedical Engineering, University of Michigan, Ann Arbor, Michigan 48109*

L. Jay Guo

*Department of Electrical Engineering and Computer Science, University of Michigan, Ann Arbor, Michigan 48109*

Matthew O'Donnell

*Department of Bioengineering, University of Washington, Seattle, Washington 98195*

(Received 31 May 2007; accepted 21 July 2007; published online 14 August 2007)

A broadband all-optical ultrasound transducer has been designed, fabricated, and tested for high-resolution ultrasound imaging. It consists of a two-dimensional gold nanostructure on a glass substrate, followed by a 3  $\mu\text{m}$  polydimethylsiloxane layer and a 30 nm gold layer. The signal to noise ratio of a pulse-echo signal is over 10 dB in the far field of the transducer, where the center frequency is 40 MHz with  $-6$  dB bandwidth of 57 MHz. The potential for high-frequency ultrasound arrays using this technology is demonstrated using multiple measurements from the transducer to image a 25  $\mu\text{m}$  diameter wire. © 2007 American Institute of Physics.

[DOI: [10.1063/1.2771058](https://doi.org/10.1063/1.2771058)]

High-frequency ultrasound ( $>30$  MHz) has been widely used for various imaging applications, including ophthalmology,<sup>1,2</sup> dermatology,<sup>3,4</sup> intravascular imaging, and small animal imaging.<sup>5</sup> At present, high-frequency acoustic microscopy uses mechanical scanning of a single element transducer, where the low  $f/\lambda$  numbers of these transducers severely restrict the depth of field, making it very difficult to make high quality images of a three-dimensional (3D) volume. Thus, two-dimensional (2D) arrays are highly desired for *in vivo*, dynamically focused 3D imaging at high frame rates. However, high-frequency arrays are extremely difficult to build with conventional piezoelectric transducers<sup>6–8</sup> and are not available for routine use, where the major problems include dicing piezoceramics to micron scale elements, electrical connections, and crosstalk between elements. Developing new transducer technologies is needed to overcome these difficulties.

Optoacoustic arrays relying on optical generation<sup>9–12</sup> and detection<sup>13–16</sup> of ultrasound have been studied for decades as an alternative to piezoelectric technologies. Instead of electronic signals, two laser beams are used as input/output, one for generation and the other for detection. The most attractive feature of optoacoustic arrays is that the size and spacing of each array element are defined by the focal spot of a laser beam; thus they can be easily reduced to several microns using conventional optics. Also, an array can be easily formed by splitting the laser beam onto an array of focused spots, avoiding the trouble of dicing the transducing surface or making any electrical connections.

The most common mechanism of optical generation of ultrasound is the thermoelastic effect.<sup>10–12</sup> A typical configuration focuses a laser pulse onto a light absorbing film deposited on a transparent substrate. Optical absorption rapidly heats up a localized volume in the film, where thermal ex-

pansion launches an acoustic wave into the overlying sample. The current state of the art optoacoustic transmitter<sup>12</sup> uses polydimethylsiloxane (PDMS) as polymer bulk, and a 2D array of gold nanoparticles as optical absorber, which produces sufficient acoustic power over a bandwidth of 100 MHz.

The most effective method of optical detection of ultrasound utilizes an etalon structure,<sup>14,15</sup> which, also known as a Fabry-Perot interferometer, consists of a polymer layer sandwiched between two optical reflectors. Light incident from an external source undergoes multiple beam interference in the etalon and produces a reflected signal intensity highly sensitive to the optical path length near the resonance wavelength. Acoustic waves propagating through the etalon modulate the cavity length, which in turn changes the reflected optical intensity; thus, the acoustic pressure can be measured by recording the intensity change of the reflected signal. Etalon sensitivity is comparable to a piezoelectric transducer of equivalent size.

Both optoacoustic transmitters and receivers have been significantly improved during the past decade and are mature enough to be integrated into a single device for practical imaging applications. In this letter, we present the first all-optical ultrasound transducer combining optoacoustic generation and detection.

To fabricate this device, a 200 nm thick polymer layer, with 2D arrangements of air holes spaced every 200 nm, is first fabricated on a glass substrate using laser interference lithography and nanoimprint lithography.<sup>17,18</sup> Each hole is 200 nm deep and  $126 \times 111 \text{ nm}^2$  in cross section. A scanning electron microscope (SEM) picture of the top view is shown in Fig. 1(a). A 20 nm layer of gold is then deposited on top of the imprinted polymer structure using an electron beam evaporator. Figure 1(b) shows a sketch of the side view of this gold nanostructure, which contains the gold nanoparticles at the bottom of the air holes as well as the gold layer on top of the polymer layer. A 3  $\mu\text{m}$  thick PDMS layer,

<sup>a)</sup>Electronic mail: yanghou@eecs.umich.edu

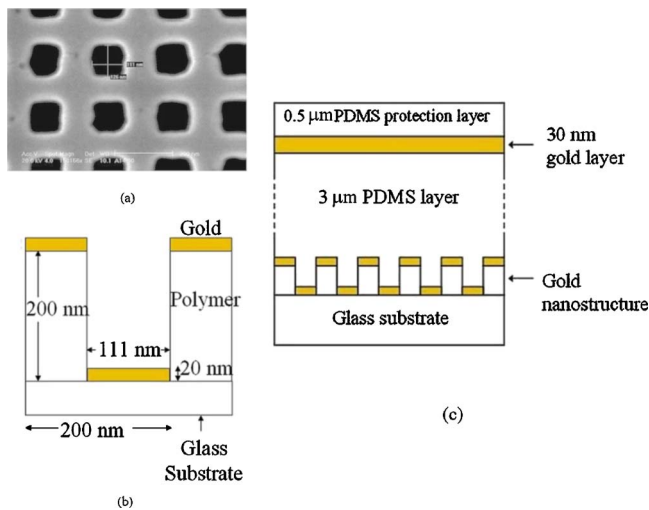


FIG. 1. (Color online) (a) SEM picture of the top view of 2D air holes in polymer. (b) Sketch of the side view of the gold nanostructure. (c) Sketch of the side view of the all-optical transducer.

followed by a 30 nm continuous gold layer, is then fabricated on top of the nanostructure. As a final step, an additional 0.5  $\mu\text{m}$  thick PDMS layer is spin cast over the entire device for protection. A sketch of the side view of the structure is shown in Fig. 1(c).

The unique optical properties of the gold nanostructure define the operating principle of the integrated transducer. The gold nanoparticles in the structure serve as efficient optical absorbers because surface plasmons localized around the particles strongly absorb light at a resonant wavelength,<sup>19,20</sup> determined to be about 780 nm for our structure. As a result, when a laser pulse at 780 nm is focused onto the gold nanostructure, over 30% of the incident optical energy is absorbed and then rapidly transferred to PDMS for ultrasound generation. On the other hand, the gold nanostructure reflects over 90% of the optical energy at wavelengths far from resonance. Thus, the gold nanostructure, together with the 30 nm thick gold layer and the PDMS layer in between, forms an etalon for ultrasound detection, where a cw laser at around 1500 nm is used as the probing optical beam.

As a first test of this device, a simple pulse-echo experiment is performed using the setup shown in Fig. 2. The optoacoustic transducer device is mounted at the bottom of a water tank. The pulsed laser excitation source is a commercial high energy solid state laser with tunable wavelength (Surelite, with OPO Plus, Continuum, Inc.), which produces a 5 ns laser pulse at a wavelength of 780 nm. The beam is

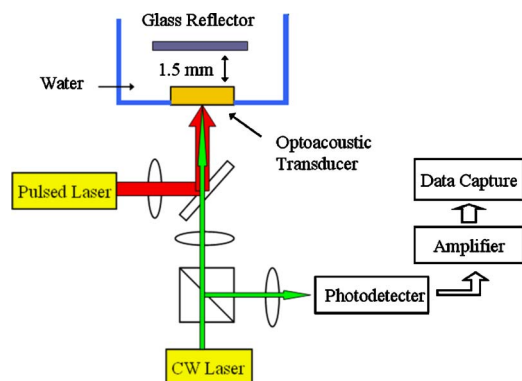


FIG. 2. (Color online) Setup of the pulse-echo experiment.

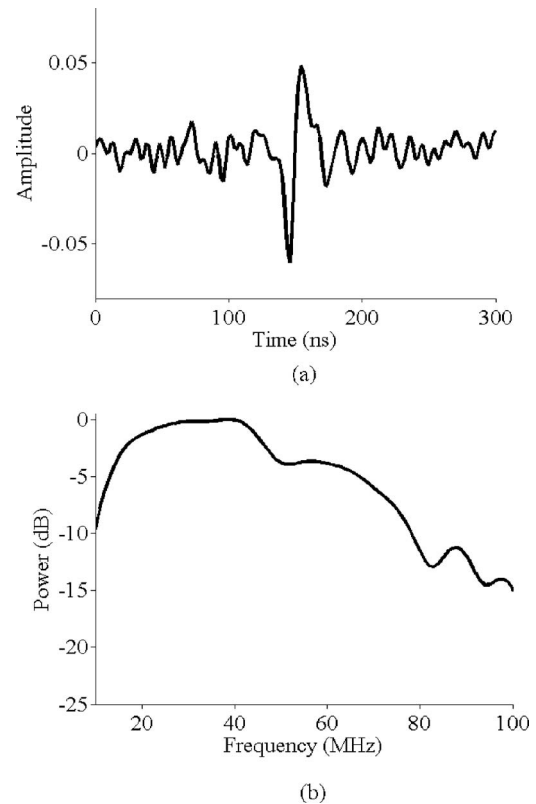


FIG. 3. (a) Single-shot pulse-echo signal. (b) Spectrum of the averaged pulse-echo signal.

coupled into a multimode fiber with core size of 50  $\mu\text{m}$ , output through a collimator, and then focused onto a 70  $\mu\text{m}$  spot on the gold nanostructure film with energy of about 1  $\mu\text{J}/\text{pulse}$  (fluence of 26  $\text{mJ}/\text{cm}^2$ ). The generated acoustic waves are launched into the water and reflected back from a glass slide aligned parallel to the etalon surface and placed about 1.5 mm away. A cw laser beam at 1500 nm with power of 4 mW is focused onto a concentric 20  $\mu\text{m}$  spot to detect the pulse-echo ultrasound signal. Reflected light is collected using an amplified InGaAs photodiode.

Figure 3(a) shows single shot acquisition of the pulse-echo signal. The signal to noise ratio (SNR) is measured to be over 10 dB for this experiment in which only a very small fraction of the transmitted acoustic power is captured by the 20  $\mu\text{m}$  diameter receive aperture. The acoustic pressure increases linearly with the optical energy absorbed by the gold nanostructure, thus the SNR can be further improved with higher optical power. The ultimate acoustic pressure available is determined by the thermal damage threshold of the structure, measured to be 25  $\mu\text{J}/\text{pulse}$  delivered to a spot size of 25  $\mu\text{m}$  (Ref. 11) (fluence of 5.1  $\text{J}/\text{cm}^2$ ), about a factor of 200 higher fluence than that used in our experiment. Thus, the SNR of a single shot pulse-echo signal for this measurement geometry can easily exceed 40 dB without damaging the device.

The spectrum of the pulse-echo signal, averaged 1000 times, is shown in Fig. 3(b). The center frequency is 40 MHz with  $-6$  dB bandwidth of 57 MHz. Theoretical studies have shown that the temporal profile of the generated ultrasound is proportional to the derivative of the input optical pulse.<sup>11</sup> Therefore, the center frequency and bandwidth of the pulse-echo signal are mainly determined by the incident laser pulse, as well as the frequency response of the etalon. The most straightforward approach to achieve higher center fre-

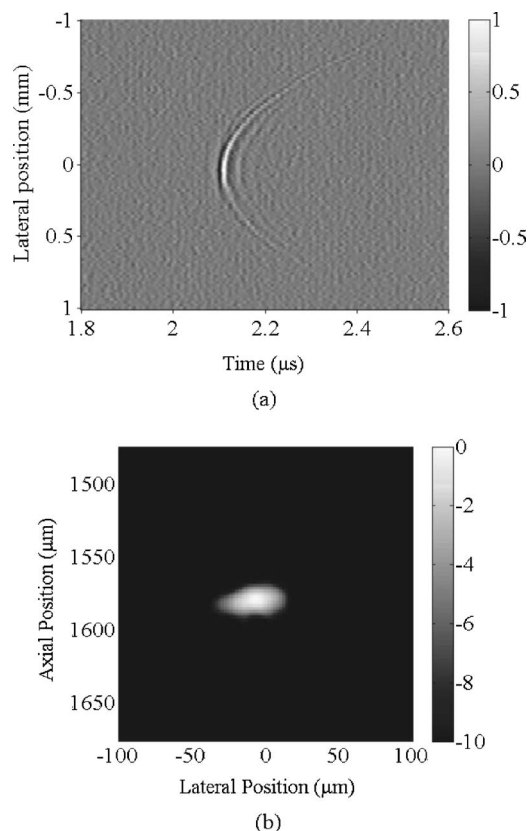


FIG. 4. (a) Wave field plot of the detected acoustic field (b) reconstructed image.

quency and broader bandwidth is to use a shorter pulse. Also, the etalon shows  $-7$  dB attenuation at 100 MHz compared to below 20 MHz. The frequency response of the etalon is directly determined by the thickness of the polymer bulk and can be greatly improved by further reducing the overall thickness of the structure. When a 2 ns laser pulse is used instead of a 5 ns one, combined with a thinner etalon, the bandwidth is expected to be enhanced to over 100 MHz.

To demonstrate the ultrasound imaging capabilities of this optoacoustic transducer, a 25  $\mu\text{m}$  diameter metal wire is used as imaging target, replacing the glass slide in the setup shown in Fig. 2. A one-dimensional (1D) synthetic aperture is formed by mechanically scanning the wire by a total distance of 2 mm with 20  $\mu\text{m}$  step separation. At each position, the signal is averaged 100 times before recording. Figure 4(a) shows a wave field plot of the detected acoustic field. Bandpass filtering (25–85 MHz) and demodulation are applied to these data, and then conventional array beam forming is performed to reconstruct the image. The  $-6$  dB axial resolution is determined to be 19  $\mu\text{m}$ , smaller than the actual wire diameter but consistent with the bandwidth of the pulse suggesting that only the echo from the wire surface contributes to the image. The  $-6$  dB lateral resolution is 38  $\mu\text{m}$ , representing about one acoustic wavelength at the 40 MHz center frequency. To improve image quality, a smaller optoacoustic transmission element size is highly desired. Currently, the element size is about 70  $\mu\text{m}$ , several times the acoustic wavelength at high frequencies. Reducing the element size to 20  $\mu\text{m}$  would significantly improve the divergence of the radiation pattern, which ultimately helps produce higher-resolution images.

At this stage, the imaging target is mechanically scanned to produce an equivalent 1D synthetic array. However, simultaneous detection of all elements in an array system is required for real-time imaging applications. This can be realized by splitting both the ultrasound generation and detection beams into an array of focused spots on the surface of the gold nanostructure. We propose to use a graded index fiber bundle for simultaneous illumination and detection. Typically, a fiber bundle contains several thousand individual light guides; each has a diameter of 10  $\mu\text{m}$ , and the spacing is also about 10  $\mu\text{m}$ . The laser power should also be increased corresponding to the total number of elements used, which can be done using erbium doped fiber amplifiers. Meanwhile, a photodiode array needs to be constructed to collect reflected light from each individual array element.

In summary, we have designed, fabricated, and tested the first all-optical ultrasound transducer. The pulse-echo signal displays good SNR and excellent bandwidth, both of which can be further improved with proper modifications to our system. High-resolution ultrasound imaging has been demonstrated using a 1D synthetic aperture. Future work includes optimizing the gold nanostructure for maximal optical absorption at the resonance wavelength and expanding a single transducer element to an array system for real-time imaging.

This work is supported in part by NIH under Grant Nos. EB003455, EB003449, and EB004933. The author thank the Resource Center for Medical Ultrasonic Transducer Technology at the University of Southern California for supplying the high-frequency piezoelectric transducers.

- <sup>1</sup>G. R. Lockwood, D. H. Turnbull, D. A. Christopher, and F. S. Foster, *IEEE Eng. Med. Biol. Mag.* **15**, 60 (1996).
- <sup>2</sup>D. J. Coleman, R. H. Silverman, A. Chabi, M. J. Rondeau, K. K. Shung, J. Cannata, and H. Lincoff, *Ophthalmology* **111**, 1344 (2004).
- <sup>3</sup>D. H. Turnbull, B. G. Starkoski, K. A. Harasiewicz, J. L. Semple, L. From, A. K. Gupta, D. N. Sauder, and F. S. Foster, *Ultrasound Med. Biol.* **21**, 79 (1995).
- <sup>4</sup>C. Passman and H. Ermert, *IEEE Trans. Ultrason. Ferroelectr. Freq. Control* **43**, 545 (1996).
- <sup>5</sup>F. S. Foster, M. Y. Zhang, Y. Q. Zhou, G. Liu, J. Mehi, E. Cherin, K. A. Harasiewicz, B. G. Starkoski, L. Zan, D. A. Knapik, and S. L. Adamson, *Ultrasound Med. Biol.* **28**, 1165 (2002).
- <sup>6</sup>T. A. Ritter, T. R. Shrout, R. Tutwiler, and K. K. Shung, *IEEE Trans. Ultrason. Ferroelectr. Freq. Control* **49**, 217 (2002).
- <sup>7</sup>J. O. Fiering, P. Hultman, W. Lee, E. D. Light, and S. W. Smith, *IEEE Trans. Ultrason. Ferroelectr. Freq. Control* **47**, 764 (2000).
- <sup>8</sup>J. M. Cannata, J. A. Williams, Q. Zhou, T. A. Ritter, and K. K. Shung, *IEEE Trans. Ultrason. Ferroelectr. Freq. Control* **53**, 224 (2006).
- <sup>9</sup>R. M. White, *J. Appl. Phys.* **34**, 3559 (1963).
- <sup>10</sup>T. Buma, M. Spisar, and M. O'Donnell, *Appl. Phys. Lett.* **79**, 548 (2001).
- <sup>11</sup>Y. Hou, S. Ashkenazi, S. W. Huang, and M. O'Donnell, *IEEE Trans. Ultrason. Ferroelectr. Freq. Control* **54**, 682 (2007).
- <sup>12</sup>Y. Hou, J. S. Kim, S. Ashkenazi, M. O'Donnell, and L. J. Guo, *Appl. Phys. Lett.* **89**, 093901 (2006).
- <sup>13</sup>J. K. Thomson, H. K. Wickramasinghe, and E. A. Ash, *J. Phys. D* **6**, 677 (1973).
- <sup>14</sup>P. C. Beard and T. N. Mills, *Appl. Opt.* **35**, 663 (1996).
- <sup>15</sup>J. D. Hamilton and M. O'Donnell, *IEEE Trans. Ultrason. Ferroelectr. Freq. Control* **45**, 216 (1998).
- <sup>16</sup>S. Ashkenazi, Y. Hou, T. Buma, and M. O'Donnell, *Appl. Phys. Lett.* **86**, 134102 (2005).
- <sup>17</sup>S. W. Ahn, K. D. Lee, J. S. Kim, S. H. Kim, S. H. Lee, J. D. Park, and P. W. Yoon, *Nanotechnology* **16**, 1874 (2005).
- <sup>18</sup>L. J. Guo, *J. Phys. D* **37**, 123 (2004).
- <sup>19</sup>S. Link and M. A. El-Sayed, *Int. Rev. Phys. Chem.* **19**, 409 (2000).
- <sup>20</sup>W. Gotschy, K. Vonmetz, A. Leitner, and F. R. Aussenegg, *Opt. Lett.* **21**, 1099 (1996).